NANOSYSTEMS: PHYSICS, CHEMISTRY, MATHEMATICS, 2019, 10 (1), P. 76–85

Injectable ultra soft hydrogel with natural nanoclay

V. S. Molchanov, M. A. Efremova, T. Yu. Kiseleva, O. E. Philippova
Department of Physics, Lomonosov Moscow State University, Leninskie Gory, 1, bld. 2, Moscow, 119991, Russia
molchan@polly.phys.msu.ru

PACS 82.70.Uv. 82.70.Dd **DOI 10.17586/2220-8054-2019-10-1-76-85**

Soft hydrogels based on a transient network of wormlike surfactant micelles containing bentonite nanoclay tactoids as physical cross-links were developed. The network was composed of mixed micelles of nontoxic zwitterionic surfactant oleylamidopropyldimethylcarboxybetaine and an anionic surfactant sodium dodecyl sulfate. It was demonstrated that before nanoclay addition the solution has pronounced viscoelastic properties with zero-shear viscosity of 100 Pa s and plateau modulus around 7 Pa, which were attributed to the formation of an entangled micellar network. The solution demonstrated pronounced shear thinning behavior provided by the elongation of wormlike micellar chains in flow direction. Upon addition of non-exfoliated nanoclay particles, the zero-shear viscosity increases by an order of magnitude, while the useful property of shear-induced thinning is retained. Oscillation amplitude tests show that viscoelastic fluid becomes hydrogel upon addition of nanoclay, because elastic response was observed even at large stress amplitudes. This behavior was attributed to the formation of nanoclay-wormlike micelles junctions. Prepared soft hydrogel is a promising candidate for injection applications, because of its self-assembled structure providing pronounced shear-thinning behavior and fast recovery of rheological properties at rest. In this nanocomposite material, nanoclay tactoids strengthen the hydrogels and can serve as reservoirs for the delivery of various substances.

Keywords: surfactant, wormlike micelles, rheology, nanoclay, bentonite, hydrogel.

Received: 15 November 2018

Revised: 29 January 2019

1. Introduction

Injectable nanocomposite hydrogels represent an ever-growing class of nanomaterials possessing a unique combination of physical and chemical properties. For injection applications, the hydrogels should demonstrate a shear-thinning behavior resulting in a significant decrease in viscosity when subjected to shear strain and a fast recovery of the initial state, when the deformation is no longer applied. Such hydrogels can be used as control delivery systems since they can be delivered in a minimally *invasive* manner because the final form and shape are defined by the space into which they are injected.

Injectable hydrogels can be based either on polymer network or on self-assembled network of wormlike surfactant micelles (WLMs). Polymer hydrogels are classically defined as three-dimensional, water-swollen polymer networks formed as a result of physical or chemical cross-linking [1, 2]. For injectable hydrogels application physically cross-linked polymer networks are preferred. They are disrupted under shear deformation during injection and then reassembled at rest due to recovery of noncovalent cross-links between the macromolecules. To provide additional functionality to the matrix the hydrogels can contain delivery vehicle components, for instance, nanoclay tactoids, which make them very promising for drug delivery and tissue engineering applications [3–5].

Another type of injectable hydrogels is based on WLMs [6–9]. Such micelles are often compared with polymers and have even been given the name of living polymers [10–12], because they incessantly break and recombine. With increasing surfactant concentration, solutions of WLMs become viscoelastic and at certain conditions, a transient network of entangled micellar chains is formed. Such a network possesses gel-like properties. In particular, its rheological properties demonstrate plateau modulus, low values of loss factor and pronounced shear- or stress-thinning behavior. At the same time, under high deformation, the micellar chains are disrupted, which induces a much more pronounced drop of viscosity than the disruption of physical cross-links in polymer gels [12, 13], which is advantageous for injection applications. The disrupted micellar chains are completely recovered due to restoration of non-covalent bonds between surfactant molecules within the micelles [12]. Thus, WLM-based hydrogels are promising candidates for the preparation of injectable systems.

Properties of the WLM network can be modified by nanoparticles. Until now, only spherical inorganic particles were dispersed within WLM network [14–20]. It was shown that these particles can significantly increase the rheological properties. For instance, near the overlap concentration of WLMs silica nanoparticles incorporated within similarly charged WLM solutions [15] induced liquid to viscoelastic fluid transition. This was explained by the formation of micelle-nanoparticle junctions as a result of binding of the WLMs to the layer of surfactant adsorbed on the particle's surface [15]. It was suggested that the WLMs are connected to surfactant layer on the

particle surface by their end-caps because these parts are energetically less favorable in comparison with cylindrical central parts of the micelles. Similar results were obtained for silica nanoparticles oppositely charged with respect to WLMs [14, 18]. At the same time, addition of particles into dense WLM network either decreased rheological properties or did not significantly alter them [14, 18].

In addition to silica nanoparticles, some functional nanoparticles were incorporated into WLM networks including pyroelectric [16] and magnetic particles [17, 19, 20]. Introduction of pyroelectric particles made the hydrogel sensitive to temperature variation. Heating increased the charge on the surface of particles thereby strengthening their interaction with oppositely charged surfactant micelles and enhancing the rheological properties [16]. In their turn, magnetic particles imparted magnetoresponsive properties to WLM hydrogel [17, 19, 20]. The aggregation of particles into chain-like/column structures because of magnetization resulted in a solid-like behavior even in rather low magnetic fields and at small volume fraction of particles, indicating the weak restrictions imposed by the matrix on the reorganization of particles in the field, which can be due to the self-assembled structure of the micellar network [19].

Thus, many types of particles were incorporated within WLM network but such systems were never tested for injection purposes. This gap is filled in the present paper. Moreover, instead of spherical particles we use plate-like particles of natural nanoclay bentonite. We suggest that large surface area of such particles will additionally stimulate the formation of WLM-particles junctions acting as cross-links in the network. Also, the interior volume of these particles is quite promising for the incorporation and further delivery of different substances [21, 22].

For the preparation of the WLM hydrogel, the nontoxic zwitterionic surfactant oleylamidopropyldimethylcarboxybetaine (OB) was used. This surfactant can make transient network of long WLMs, as was shown recently [23, 24]. Betaines demonstrate a strong synergism when mixed with anionic surfactant [25], in particular, sodium dodecyl sulfate (SDS) [26]. For this reason, in the present paper, a small amount of SDS is added to OB. Zwitterionic surfactants are the most eco-friendly and biocompatible type of the surfactants widely applied in different cosmetic products. To the best of our knowledge, soft nanocomposites based on the zwitterionic surfactant were not previously investigated.

Thus, the present paper is devoted to the preparation and study of soft nanocomposite hydrogels based on network of WLMs composed of zwitterionic and anionic surfactants with embedded plate-like bentonite nanoclay particles. It is shown that nanoparticles significantly enhance the rheological properties of WLM hydrogel, acting as physical cross-links between micellar chains. It was demonstrated that the prepared nanocomposite hydrogels possess promising properties for injection applications.

2. Experimental section

2.1. Materials

Zwitterionic surfactant OB (Fig. 1) with molar mass 450.5 g/mol and density of 1.1 g/cm^3 was purchased from SPF NIIPAV (Russia) as a solution containing 29.0 wt. % OB, 0.5 wt. % oleylamidopropyldimethylamine, 4.0 wt. % sodium chloride, 17.0 wt. % isopropanol, and 49.5 wt. % water. To recover the solids the solvents were removed by lyophilization. The complete removal of isopropanol was confirmed by 1H NMR spectroscopy. The resulting dried solid contained 85.0 wt. % OB (surfactant), 1.44 wt. % oleylamidopropyldimethylamine, and 13.56 wt. % sodium chloride. The carboxylic group of OB has pK = 2 [27], at the pH range under study (pH = 11÷11.5) it is always charged and therefore the OB molecules are in the zwitterionic form. The ratio between sodium chloride and OB is stoichiometric, since sodium and chloride ions are counterions of the charged groups of the surfactant. The third component of the mixture – oleylamidopropyldimethylamine is a byproduct of the synthesis OB. Note that the molar ratio between oleylamidopropyldimethylamine and OB surfactant is very small (1:51), and at the experimental conditions (pH = 11÷11.5) the amine is uncharged, therefore it cannot appreciably affect the behavior of the OB surfactant.

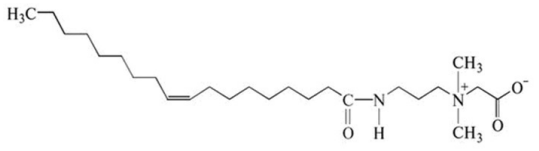

FIG. 1. Chemical structure of zwitterionic surfactant oleylamidopropyldimethylcarboxybetaine (OB)

The anionic surfactant SDS, with molar mass of 265 g/mol and density of 1.0 g/cm^3 was purchased from Helicon. Bentonite nanoclay with density of 2.4 g/cm^3 was provided by Sigma-Aldrich. Its specific surface area is 63 m^2/g [28]. The surface of bentonite nanoclay platelets contains Al–OH, Mg–OH and Si–OH functional groups [29]. At pH range under study (pH = 11 – 11.5), the clay carries negative charge both on the face and at the edge of a platelet [30]. Sodium hydroxide with purity 85 % and molar mass 56.11 g/mol was purchased from Riedel-de Haen. Double distilled water purified on Milli-Q Millipore Waters was used as a solvent.

2.2. Organoclay preparation

It is well known [31–34] that clay can adsorb ionic surfactants both on the external surface and into the interlayer region of tactoids (stacks of parallel clay platelets). As a result, the exchangeable ions can be transferred from the tactoids to the solution. Therefore, when clay is added to a solution of WLMs, the effective concentration of a surfactant in the solution can decrease, whereas the concentration of ions can increase. To prevent these effects, we prepared organoclay saturated with the surfactant, thus ensuring that the clay will not adsorb more surfactant from the solution.

Three different types of organoclays were prepared: (i) clay saturated with only SDS (anionic organoclay), (ii) clay saturated with only OB (zwitterionic organoclay), and (iii) clay saturated with both these surfactants (mixed organoclay). To prepare each type of clay, the bentonite (4 wt. %) was added to water containing an excess of surfactant (0.6 wt. %). The resulting dispersions were stirred with a magnetic stirrer for two days for complete intercalation of surfactant into the clay. Then saturated clay was separated from the surfactant solution by centrifugation (10 min at a speed of 5000 rpm) and rinsed several times with distilled water. As was demonstrated previously [31–34], after these operations the intercalated surfactant remains between the clay platelets. The saturated organoclay thus prepared was dried for 3 days at 50 °C and then ground in an agate mortar. As was demonstrated previously [34], after these operations the intercalated surfactant remains between the clay platelets.

2.3. Characterization methods

2.3.1. Transmission electron microscopy (TEM). TEM experiments were performed on transmission electron microscope LEO912 AB OMEGA. To prepare samples for TEM examination, a drop of 0.01 wt. % aqueous dispersion of clay was deposited on the grid and dried.

2.3.2. X-ray diffraction. Powder X-ray diffraction patterns were recorded on a Empyrean PANalytical diffractometer in θ-2θ geometry using CuKα radiation ($\lambda_{k\alpha}(\mathrm{Cu}) = 0.15406$ nm). Patterns were processed using HighScore software and structure database JSPDS.

2.3.3. Elemental analysis. CHN elemental analysis of the modified nanoclay samples was performed with Vario Micro Cube Elementar Analyzer (Germany). The technique is based on the quantitative flash combustion method. In the combustion process (at ca. 1000 °C), carbon is converted to carbon dioxide; hydrogen to water; nitrogen to nitrogen gas/oxides of nitrogen. The gases are then passed through the absorbent traps in order to leave only carbon dioxide, water, nitrogen and then analyze them.

2.3.4. Rheology. Experiments were performed on rheometer Anton Paar Physica MCR301 at 25 °C. Steady shear measurements were carried out by setting shear stress σ and measuring shear rate $\dot{\gamma}$. Oscillation amplitude tests were carried out at a fixed frequency of 1 rad/s. Recovery test was carried out at fixed frequency of 6 rad/s and step-like amplitudes of 0.1 and 20 Pa, which correspond respectively to linear and non-linear regimes. In the last case, the amplitude was so high that the network should be disrupted.

In all experiments, the cone-plane measuring cell CP50-1 with diameter 49.973 mm, angle 10 and sample volume 0.78 ml was used.

3. Results and discussion

3.1. Clay and organoclay characterization

The nanoclay particles were visualized by TEM. The image of bentonite is presented on Fig. 2. Similar TEM images were obtained for three different types of organoclay. They show that the average size of clay platelets is around 100 nm (Fig. 2, left). The platelets are aggregated in tactoids (Fig. 2, right) that is the interaction with surfactants does not induce a full exfoliation of clay layers. This suggests rather weak adsorption of the surfactants by the clay.

To estimate the amount of the adsorbed surfactants, elemental analysis was employed. The estimation was made taking into account that all surfactants have carbon atoms, while clay itself does not contain them. In addition, among the surfactants under study, the zwitterionic surfactant has nitrogen. The results of estimation

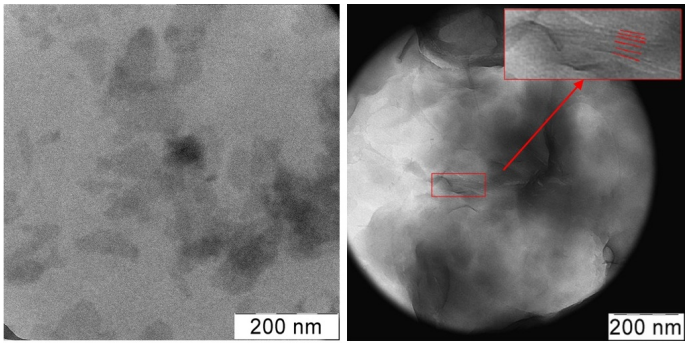

FIG. 2. TEM micrographs of bentonite. Magnified image (inset) demonstrates an inner structure of clay tactoid

TABLE 1. Characteristics of the clay samples

Clay	Interlayer space d_{001}, nm	Amount of adsorbed surfactant	
		in mmol/g	in % of CEC
Bentonite	1.301	0	0
Organoclay with anionic surfactant	1.437	0.08	1.6
Organoclay with zwitterionic surfactant	1.459	0.27	8.0
Organoclay with mixed anionic and zwitterionic surfactants	1.356	0.03	0.7

are given in Table 1. The obtained values represent the total amount of the surfactant molecules intercalated within tactoids and adsorbed on their surface. It is seen that among the surfactants under study, the zwitterionic surfactant is more effectively adsorbed by the clay. Its adsorption is provided by electrostatic and hydrophobic interactions [31, 32]. However, even in this case, the amount of the adsorbed surfactant is much smaller than the cation exchange capacity (CEC) of bentonite equal to 90 – 110 mmol/100 g [29, 34] usually characterizing the amount of intercalated surfactant molecules which can exfoliate tactoids as a result of the removal of all exchangeable ions [31, 34]. This value can be achieved by cationic surfactants, which strongly bind on oppositely charged clay surfaces. As seen from Table 1, the adsorption of zwitterionic surfactant reaches only 8 % of CEC. As to anionic surfactant, its adsorption is even smaller (1.6 % of CEC), which may be attributed to electrostatic repulsion with similarly charged clay surface. Some amount of anionic surfactant adsorption, which is still occurs on the clay, may be due to hydrophobic interactions. By contrast, in the case of zwitterionic surfactant, the electrostatic attraction should also contribute to the adsorption resulting in the increase of the adsorption capacity. From Table 1, one can see that mixed organoclay contains the lowest amount of surfactant. Probably, this pair of surfactants prefers to form mixed micelles in the solution rather than to intercalate into the clay.

With the surfactant intercalation, the space between the clay layers increases due to the large size of the surfactant molecules [32]. To measure the gap between the clay platelets, X-ray diffraction (XRD) analysis was performed. XRD patterns of bentonite and three types of organoclay: anionic, zwitterionic and mixed are presented in Fig. 3. Analysis of the peaks using the database for clays JSPDS shows that the closest structure, which describes the position of the diffraction peaks is montmorillonite, the main component of bentonite. The diffraction patterns show that the positions of these peaks are similar for bentonite and organobentonite. Reflection peak (001) at the lowest angle corresponds to a distance between the platelets. Other peaks correspond to the inner crystalline structure of the platelets, and their position does not depend on the presence of surfactant molecules between the platelets. As to the (001) peak, in organoclays it is shifted towards lower angles (Fig. 3), pointing to an increase in the interlayer distances d, which can be estimated from the formula $d = \dfrac{\lambda}{2\sin\theta}$, where $\lambda = 0.154$ nm is the wavelength of $K\alpha$-radiation of copper.

The interlayer distance d values are summarized in Table 1. It is seen that for unmodified bentonite, the distance d is 1.301 nm, and it increases for organoclays, which suggests the intercalation of surfactants in the interlayer space of the clay. From Table 1, one can see that the most pronounced increase of d_{001} is observed

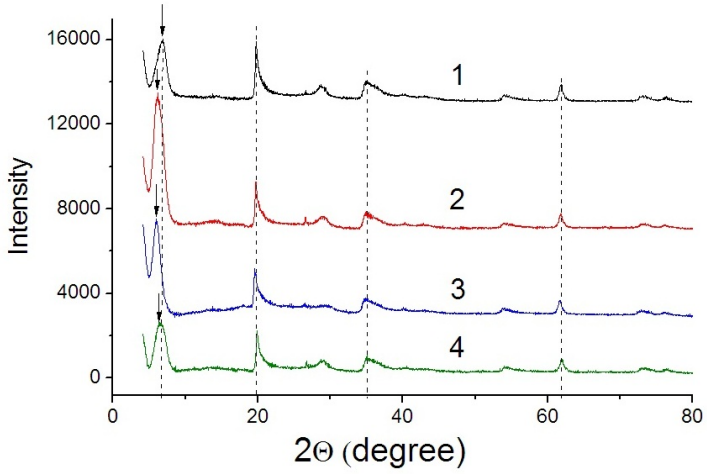

FIG. 3. XRD patterns of bentonite (top curve 1) and different organoclays: anionic (2), zwitterionic (3) and mixed (4). For clarity the intensity of the curves 1, 2, 3 was multiplied by 40, 20 and 10, respectively

for zwitterionic organoclay, which is more saturated with surfactant than other organoclays. Mixed organoclay contains the lowest amount of surfactant and the gap between platelets is increased only slightly. As to anionic clay, surprisingly its interlayer distance is increased significantly compared to untreated bentonite, whereas the amount of adsorbed surfactant is rather low. This may be due to the electrostatic repulsion between the clay and the intercalated surfactant.

It is important to note that in all types of organoclay, the intercalation of surfactant does not lead to exfoliation, as the peak corresponding to periodic packing of platelets in tactoids saves its shape. Most of the observed tactoids are composed of 6 – 10 clay platelets, therefore, the height of the tactoids is nearly 10 – 15 nm. Their axial ratio is about 1:8, because the average size of the clay platelets is around 100 nm.

Thus, it was shown that anionic and zwitterionic surfactants intercalate into the clay tactoids, but in small amounts, so that exfoliation does not occur. It suggests that the organoclay, which is used as a nanofiller of WLM network, retains the useful properties of the initial clay and it can serve e.g. as delivery vehicle for various substances embedded between the platelets.

3.2. Viscoelasticity of WLM networks with embedded nanoclay particles

Stable suspensions of mixed organoclay in viscoelastic surfactant solutions were prepared. For this purpose, 0.1 wt. % organoclay saturated with mixed surfactant was added to an aqueous solution of the same surfactant mixture (2 wt. % of zwitterionic surfactant OB and 0.1 wt. % SDS), which was used for the preparation of the organoclay. The concentration of organoclay under study was much less than the percolation threshold of the clay platelets (around 3 – 5 wt. %). At 0.1 wt.% content of the nanoclay, the sample was homogeneous and stable for a long period of time (for at least 6 months).

Before the addition of the organoclay, the surfactant solutions represented viscoelastic fluids. It should be noted that the 2 wt. % OB solution, even without SDS, possesses viscoelastic properties indicating to the presence of WLMs [23, 24]. At the same time, the solution of 0.1 wt. % of SDS behaves as Newtonian liquid with very low viscosity close to pure water because at this concentration SDS forms only spherical micelles. The rheological properties of the mixed OB–SDS surfactant system suggest the presence of network of entangled WLMs (Figs. 4,5), since the zero-shear viscosity is several orders of magnitude higher than that of water and the dynamic rheological data demonstrate a large region of predominantly elastic response, where the storage modulus exceeds the loss modulus $G' > G''$ [35].

The influence of organoclay on the rheological properties of mixed WLMs of surfactants was studied. Fig. 4(a) shows the viscosity as a function of shear stress before and after the addition of nanoclay particles. At low stress, for both systems, one can see a plateau corresponding to zero-shear viscosity. Above a critical shear stress value (2 Pa), the viscosity of pure surfactant system sharply drops by 5 orders of magnitude, approaching the viscosity of pure water. So pronounced shear-thinning behavior is typical for the network of entangled WLMs. It was explained by shear-induced elongation of wormlike micellar chains in flow direction [36, 37].

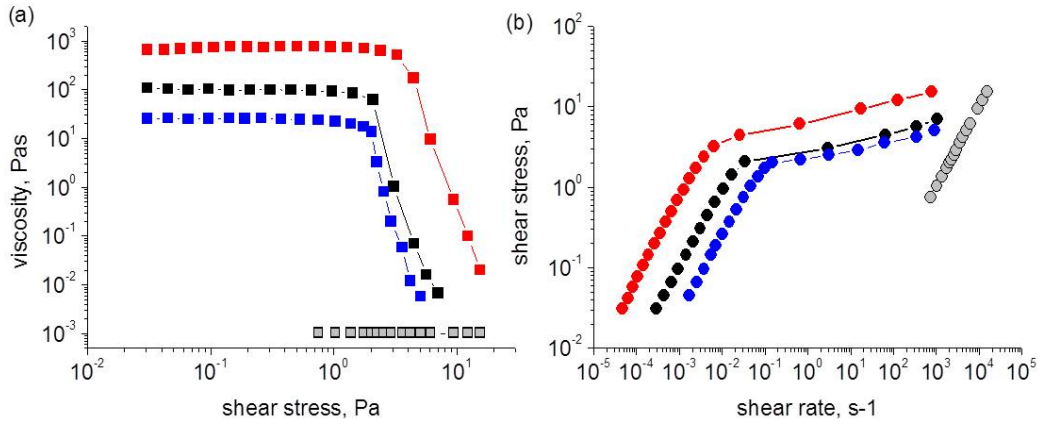

FIG. 4. Viscosity as a function of shear stress (a) and shear stress as a function of shear rate (b) for solutions of 2 wt.% zwitterionic OB (blue), 0.1 wt.% anionic SDS (grey), 2 wt.% zwitterionic OB surfactant and 0.1 wt.% anionic SDS surfactant before (black) and after (red) the addition of 0.1 wt.% bentonite

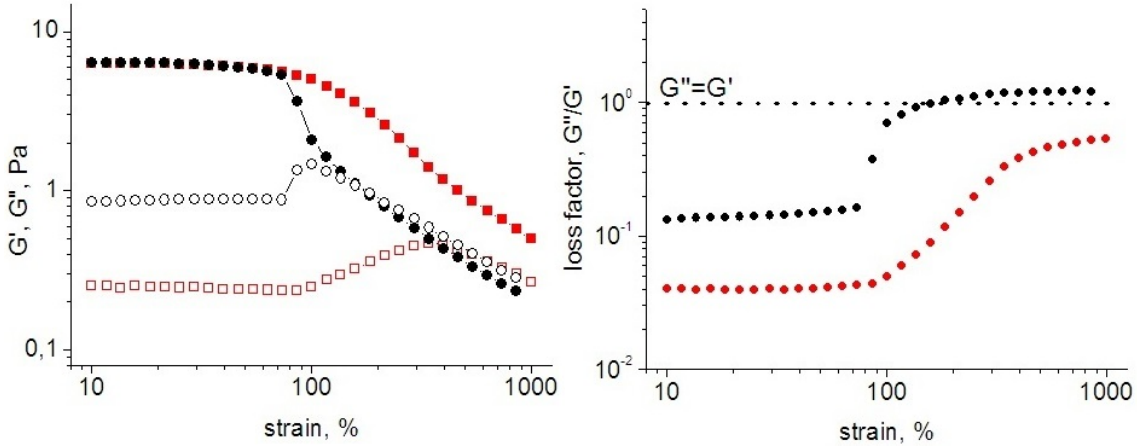

FIG. 5. Storage (filled symbols) and loss moduli (open symbols) as a function of oscillation amplitude at 1 rad/s (a) and the corresponding dependence of the loss factor for solution of 2 wt.% zwitterionic OB surfactant and 0.1 wt.% anionic SDS surfactant before (black) and after (red) the addition of 0.1 wt.% bentonite

In the presence of nanoclay particles, the overall behavior is still the same with a huge viscosity drop, but the zero-shear viscosity rises by one order of magnitude and the shear-thinning region starts from higher stress (Fig. 4(a)). The effect of nanoclay can be explained by the formation of nanoclay-WLM junctions. The particles covered by surfactant can act as physical cross-links of the WLM network similar to spherical inorganic particles [15, 17]. When organoclay is added into the surfactant network, the end-caps of WLMs as the most unfavorable parts of the micellar chains can fuse with surfactant aggregates on the particles. One can suggest that the point of the junction can slide along the nanoclay particles surface to get additional gain in entropy.

Figure 4(b) shows the shear stress as a function of shear rate before and after the addition of nanoclay particles. It is seen that very high shear rates can be achieved if we will overcome initial linear region. This is significant for the application of these gels as an injectable system. Fig. 4(b) demonstrates that in the presence of nanoclay, higher values of stresses are required to obtain the high shear rates that indicates the impact of nanoclay cross-links on the flow of the sample.

To determine the elastic response of both pure surfactant network and the nanocomposite network the oscillation stress was applied to the samples. At an angular frequency of 1 rad/s the storage G' and loss G'' moduli were measured as a function of the deformation amplitude (Fig. 5(a)). From Fig. 5(a) it is seen that at small amplitudes until 70 % in the absence of the nanoclay the storage modulus is higher than the loss modulus almost by one

order of magnitude pointing out to a gel-like behavior. The entanglements of the WLMs make three-dimensional network demonstrating such elastic response (Fig. 6 left). Moreover, these moduli do not depend on the amplitude, indicating that it is the region of linear viscoelasticity. Out of this region (i.e. at higher amplitudes), the storage modulus drops and becomes even lower than the loss modulus suggesting the transition to viscous flow state. This indicates that the number of entanglements in the WLM network decreases under action of high amplitude shear stresses.

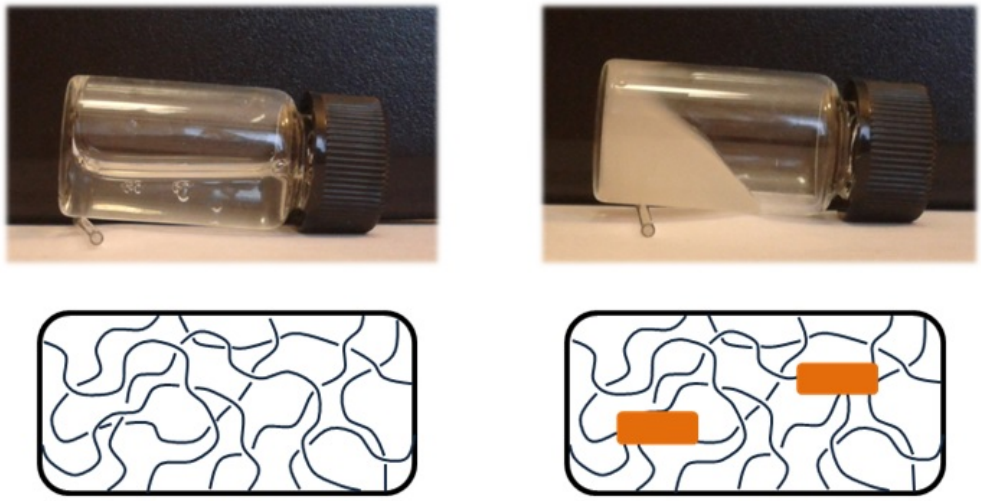

FIG. 6. Solution of 2 wt.% zwitterionic OB surfactant and 0.1 wt.% anionic SDS surfactant before (left) and after addition of 0.1 wt.% bentonite (right). The structure of the corresponding systems is shown on the schematic representations below the photos. Before the addition of nanoclay the solution contains entangled WLMs (left); after the addition of nanoclay the solution contains two types of cross-links: entanglements of WLMs and WLM/nanoclay junctions (right)

In the presence of nanoclay particles, at small amplitudes, the storage modulus retains its values, whereas the loss modulus drops significantly (Fig. 5(a)). This means that dissipated part of the response corresponding to WLM reptation motion supplemented by breaking and recombination processes becomes lower. This can be explained by the formation of additional bonds in the network due to cross-linking of the WLMs by nanoclay particles. At higher amplitudes the storage modulus decreases, but remains always higher than G'' up to as large amplitudes of deformation as 1000 %. We assume that at high amplitudes, the network partly disrupts: the number of the entanglements between the WLMs decreases, whereas the links between nanoclay and WLMs are strong enough so that the WLM/nanoclay junctions remain undisrupted providing predominantly elastic response ($G' > G''$) of the system. Thus, at low amplitudes, there are two types of cross-links in the network: entanglements between WLMs and WLM/nanoclay junctions (Fig. 6 right). With increasing amplitude, some of the entanglements disappear (since storage modulus for neat WLM network decreases), but the elastic response of the nanoclay containing network remains up to much higher amplitudes indicating that the strength of WLM/nanoclay junctions is higher than that of WLMs entanglements. Thus, nanoclay junctions in WLM network convert WLM viscoelastic fluid into soft WLM nanocomposite hydrogel.

Surprisingly, a maximum of loss modulus is observed at some oscillation amplitude both for pure surfactant and for nanocomposite networks (Fig. 5(a)). According to literature [38, 39], it can be due to the interactions between the WLMs opposing their alignment induced by the strain. For instance, similar maximum was obtained for CTAB micelles with embedded hydrotrope ions [39]. This was attributed to the formation of connections between WLMs as a result of penetration of hydrotrope into two neighboring micellar chains. The same behavior is observed in the present system without any hydrotrope ions indicating that the WLMs can interact with each other in the absence of hydrotrope salt. When clay particles are added, the maximum of loss modulus becomes more pronounced and shifts toward large amplitudes indicating to stronger links between subchains in the nanocomposite network in comparison with the pure WLM network, thus pointing out to the cross-linking of WLMs by clay particles.

Figure 5(b) shows the loss factor (G''/G') as a function of amplitude of deformation for pure WLM and nanofilled systems. The value of loss factor lower than 1 ($G''/G' < 1$) indicates gel-like state, while higher values ($G''/G' > 1$) are inherent for viscous flow state for the samples. From Fig. 5(b), it is seen that with increasing

amplitude, a gel-to-liquid transition takes place in the absence of nanoclay, whereas when nanoclay is present, a gel-like state is observed in the whole range of deformation amplitudes up to 1000 %.

Thus, bentonite nanoclay particles can be incorporated into similarly charged WLM network and induce pronounced reinforcement of the structure (Fig. 6). The observed enhancement of rheological properties indicates to the formation of particles-WML physical junctions.

3.3. Recovery test

The oscillation recovery tests were carried out both at small (0.1 Pa) and high (20 Pa) stress amplitudes at fixed angular frequency (6 rad/s) to study breaking and recovery of the nanocomposite WLM network. Fig. 7(a) shows the storage and the loss moduli as a function of time under periodic change from low (0.1 Pa) to high (20 Pa) stress amplitude actions. It is seen that initially at low stress (cycle 1) $G' > G''$ indicating to the gel state of the system, but under high stress (cycle 2) storage modulus drops by almost 3 orders of magnitude and becomes lower than the loss modulus $G' < G''$ (liquid-like state). This suggests that at high amplitudes, the network disrupts because the cross-links and wormlike subchains themselves are formed by relatively weak physical interactions. At the same time, at further switching to low stress (cycle 3) the system rapidly turns back to the gel state $G' > G''$, which can be attributed to the reassembly of the nanocomposite surfactant network. From Fig. 7(a), it is seen that the disruption of the network is faster than the recovery. Gradual growth of the storage modulus takes tens of the seconds that is close to the typical relaxation time for the WLM networks [20, 25]. Such restoring rate is comparable to the restoring rate of various injectable systems for wound healing application [5]. Fig. 7(b) demonstrates the variation of the loss factor under the same periodical action. It is seen that the loss factor jumps by 2 orders of magnitude from gel state ($G''/G' < 1$) into liquid state ($G''/G' > 1$). These high changes are more pronounced than those obtained for polymer-nanoclay hydrogel physically cross-linked by ions [5], where only cross-links are disrupted under high stress amplitudes, whereas the polymer chains remain intact. WLM-based network is more responsive to shear stress because not only cross-links, but also subchains can be disrupted under the stress. Thus, the WLM-based hydrogel have demonstrated high responsiveness to shear actions that makes it promising as an injectable system.

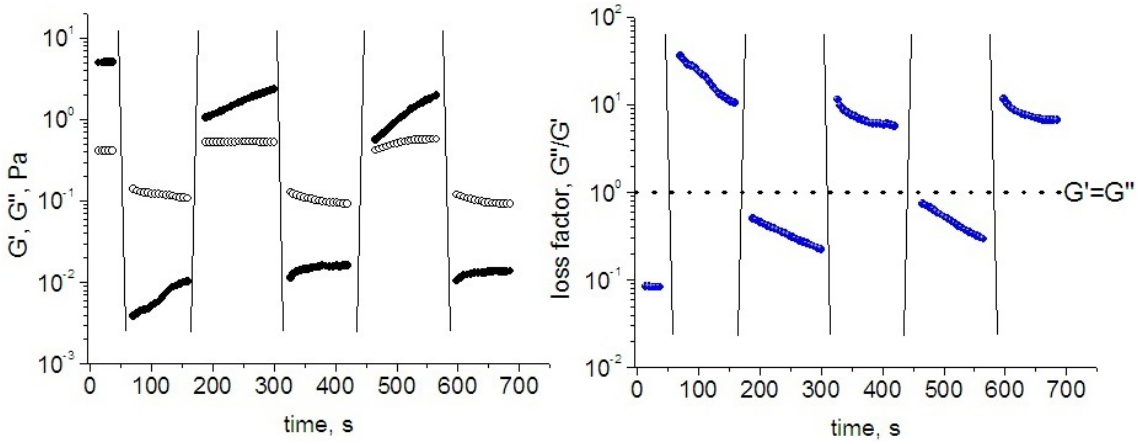

FIG. 7. Storage (filled symbols) and loss moduli (open symbols) as a function of time under periodic change of stress amplitude from 0.1 to 20 Pa at angular frequency of 6 rad/s (a) and the corresponding dependence of the loss factor (b) for solution of 2 wt.% zwitterionic OB surfactant and 0.1 wt.% anionic SDS surfactant containing 0.1 wt.% bentonite

4. Conclusions

The nanocomposite WLM-based soft hydrogels containing tactoid particles of bentonite organoclay are developed. It was found that the mixture of zwitterionic and anionic surfactant molecules adsorb only moderately on nanoclay tactoids and in much smaller amounts than the surfactant molecules taken separately. The adsorption of the surfactant molecules did not exfoliate nanoclay tactoids. A pronounced enhancement of rheological properties of transient WLM network induced by nanoclay was observed. It was explained by the formation of particle-WLM physical junctions reinforcing the network.

High zero-shear viscosity and plateau modulus of the nanoclay-WLM hydrogels at moderate stress and shear were detected, whereas significant shear- and amplitude-thinning effect at high stress was demonstrated. Shear-induced disruption of the hydrogel and further recovery were explained by reassembly of non-covalent links in WLM micelles and in nanoparticle-WLMs junctions.

The changes of rheological properties of WLM-based hydrogels induced by shear are more significant in comparison with polymer-based physical nanocomposite hydrogels. This was explained by subchain disruption of the WLM network under shear action in contrast to only cross-links disruption of polymer-based system. The observed properties make WLM-based nanocomposite hydrogels promising candidates for injectable applications, where nanoclay tactoids can be useful as delivery vehicles.

Acknowledgements

This work was supported by the Russian Science Foundation (project No. 17-13-01535).

References

[1] Philippova O.E., Khokhlov A.R. Polymer gels. In *Polymer Science: A Comprehensive reference*, vol. 1, Elsevier B.V., USA, 2012, P. 339–366.
[2] Philippova O.E., Chtcheglova L.A., Karybiants N.S., Khokhlov A.R. Two mechanisms of gel/surfactant binding. *Polymer Gels and Networks*, 1998, **6**, P. 409–421.
[3] Sharifi S., Blanquer S.B.G., Van Kooten T.G., Grijpma D.W. Biodegradable nanocomposite hydrogel structures with enhanced mechanical properties prepared by photo-crosslinking solutions of poly(trimethylene carbonate)-poly(ethylene glycol)-poly(trimethylene carbonate) macromonomers and nanoclay particles. *Acta Biomater.*, 2012, **8** (12), P. 4233–4243.
[4] Li C., Shi G. Functional gels based on chemically modified graphenes. *Advanced Materials*, 2014, **26** (24), P. 3992–4012.
[5] Lokhande G., Carrow J.K., et al. Nanoengineered injectable hydrogels from kappa-carrageenan and two-dimensional nanosilicates for wound healing application. *Acta Biomater.*, 2018, **70** (1), P. 35–47.
[6] Rehage H., Hoffmann H. Rheological properties of viscoelastic surfactant systems. *J. Phys. Chem.*, 1988, **92** (16), P. 4712–4719.
[7] Granek R., Cates M.E. Stress relaxation in living polymers: Results from a Poisson renewal model. *J. Chem. Phys.*, 1992, **96** (6), P. 4758–4767.
[8] Philippova O.E. Self-assembled networks formed by wormlike micelles and nanoparticles. In *Wormlike Micelles: Advances in Systems, Characterisation and Applications*, Soft Matter Series, 2017, **6**, P. 103–120.
[9] Shibaev A.V., Philippova O.E. Viscoelastic properties of new mixed wormlike micelles formed by a fatty acid salt and alkylpyridinium surfactant. *Nanosystems: Physics, Chemistry, Mathematics*, 2017, **8** (6), P. 732–739.
[10] Berret J.-F., Appell J., Porte G. Linear rheology of entangled wormlike micelles. *Langmuir*, 1993, **9** (11), P. 2851–2854.
[11] Dreiss C.A. Wormlike micelles: Where do we stand? Recent developments, linear rheology and scattering techniques. *Soft Matter*, 2007, **3** (8), P. 956–970.
[12] Chu Z., Dreiss C.A., Feng Y. Smart wormlike micelles. *Chem. Soc. Rev.*, 2013, **42** (17), P. 7174–7203.
[13] Khatory A., Lequeux F., Kern F., Candau S.J. Linear and nonlinear viscoelasticity of semidilute solutions of wormlike micelles at high salt content. *Langmuir*, 1993, **9** (6), P. 1456–1464.
[14] Bandyopadhyay R., Sood A.K. Effect of silica colloids on the rheology of viscoelastic gels formed by the surfactant cetyl trimethylammonium tosylate. *J. Colloid Interface Sci.,* 2005, **283**, P. 585–591.
[15] Helgeson M.E., Hodgdon T.K., Kaler E.W., Wagner N.J. Formation and rheology of viscoelastic "double networks" in wormlike micelle-nanoparticle mixtures. *Langmuir*, 2010, **26** (11), P. 8049–8060.
[16] Luo M., Jia Z., et al. Rheological behavior and microstructure of an anionic surfactant micelle solution with pyroelectric nanoparticle. *Colloids and Surfaces A: Physicochem. Eng. Aspects,* 2012, **395**, P. 267–275.
[17] Pletneva V.A., Molchanov V.S., Philippova O.E. Viscoelasticity of smart fluids wormlike micelles and oppositely charged magnetic particles. *Langmuir*, 2015, **31**, P. 110–119.
[18] Fan Q., Li W., et al. Nanoparticles induced micellar growth in sodium oleate wormlike micelles solutions. *Colloid. Polym. Sci*., 2015, **293** (9), P. 2507–2513.
[19] Molchanov V.S., Pletneva V.A., et al. Soft magnetic nanocomposites based on adaptive matrix of wormlike surfactant micelles. *RSC Adv.*, 2018, **8** (21), P. 11589–11597.
[20] Molchanov V.S., Klepikov I.A., Razumovskaya I.V., Philippova O.E. Magnetically tunable viscoelastic response of soft magnetic nanocomposites with wormlike surfactant micellar matrix. *Nanosystems: Physics, Chemistry, Mathematics*, 2018, **9** (3), P. 335–341.
[21] Hosseini F., Hosseini F., Jafari S.M., Taheri A. Bentonite nanoclay-based drug-delivery systems for treating melanoma. *Clay Minerals*, 2018, **53** (1), P. 53–63.
[22] Zhang Y., Peng M.L., et al. Emerging integrated nanoclay-facilitated drug delivery system for papillary thyroid cancer therapy. *Scientific Reports*, 2016, **6**, AN33335.
[23] Kelleppan V.T., Moore J.E., et al. Self-Assembly of long-chain betaine surfactants: effect of tail group structure on wormlike micelle formation. *Langmuir*, 2018, **34** (3), P. 970–977.
[24] McCoy T.M., King J.P., et al. The effects of small molecule organic additives on the self-assembly and rheology of betaine wormlike micellar fluids. *J Colloid Interface Sci.*, 2019, **534**, P. 518–532.
[25] Kuryashov D.A., Philippova O.E., et al. Temperature effect on the viscoelastic properties of solutions of cylindrical mixed micelles of zwitterionic and anionic surfactants. *Colloid J.*, 2010, **72**, P. 230–235.
[26] Christov N.C., Denkov N.D., et al. Synergistic sphere-to-rod micelle transition in mixed solutions of sodium dodecyl sulfate and cocoamidopropyl betaine. *Langmuir*, 2004, **20**, P. 565–571.

[27] Weers J.G, Rathman J.F., et al. Effect of the intramolecular charge separation distance on the solution properties of betaines and sulfobetaines. *Langmuir*, 1991, **7**, P. 854–867.
[28] Tayebee R., Mazruy V. Acid-thermal activated nanobentonite as an economic industrial adsorbent for malachite green from aqueous solutions. Optimization, isotherm, and thermodynamic studies. *J. Water Environ. Nanotechnol.*, 2018, **3** (1), P. 40–50.
[29] Baik M.H., Lee S.Y. Colloidal stability of bentonite clay considering surface charge properties as a function of pH and ionic strength. *J. Ind. Eng. Chem.*, 2010, **16**, P. 837–841.
[30] Yao M., Zhang X., Lei L. Removal of reactive Blue 13 from dyeing wastewater by self-assembled organobentonite in a one-step process. *J. Chem. Eng. Data*, 2012, **57** (7), P. 1915–1922.
[31] Zhu J., Qing Y., et al. Preparation and characterization of zwitterionic surfactant-modified montmorillonites. *J. Colloid Interface Sci.*, 2011, **360** (2), P. 386–392.
[32] Belova V., Mohwald H., Shchukin D.G. Ultrasonic intercalation of gold nanoparticles into a clay matrix in the presence of surface-active materials. Part II: negative sodium dodecylsulfate and positive cetyltrimethylammonium bromide. *J. Phys. Chem.*, 2009, **113**, P. 6721–6760.
[33] Yalçin T., Alemdar A., Ece Ö.I., Güngör N. The viscosity and zeta potential of bentonite dispersions in presence of anionic surfactants. *Materials Letters*, 2002, **57**, P. 420–424.
[34] Kooli F. Exfoliation properties of acid-activated montmorillonites and their resulting organoclay. Langmuir, 2009, **25** (2), P. 724–730.
[35] Molchanov V.S., Shashkina Y.A., Philippova O.E., Khokhlov A.R. Viscoelastic properties of aqueous anionic surfactant (potassium oleate) solutions. *Colloid J.*, 2005, **67** (5), P. 606–609.
[36] Lerouge S., Berret J.-F. Shear-induced transitions and instabilities in surfactant wormlike micelles. *Adv. Polym. Sci.*, 2009, **230**, P. 1–71.
[37] Molchanov V.S., Philippova O.E. Dominant role of wormlike micelles in temperature-responsive viscoelastic properties of their mixtures with polymeric chains. *J. Colloid Interface Sci.*, 2013, **394**, P. 353–359.
[38] Hyun K., Kim S.H., Ahn K.H., Lee S.J. Large amplitude oscillatory shear as a way to classify the complex fluids. *J. Non-Newtonian Fluid Mech.*, 2005, **107**, P. 51–65.
[39] Zhao Y. Rheological characterizations of wormlike micellar solutions containing cationic surfactant and anionic hydrotropic salt. *J. Rheology*, 2015, **59** (5), P. 1229–1259.